Early Glaucoma Detection using LSTM-CNN integrated with Multi Class SVM

Vijaya Madhavi Vuppu
Department of CSE, Koneru Lakshmaiah Education Foundation, Hyderabad, Telangana, India | Department of CSE, Neil Gogte Institute of Technology, Hyderabad, Telangana, India
madhavikrishnat@klh.edu.in

P. Lalitha Surya Kumari
Department of CSE, Koneru Lakshmaiah Education Foundation, Hyderabad, Telangana, India
vlalithanagesh@gmail.com (corresponding author)

Received: 11 May 2024 | Revised: 31 May 2024 | Accepted: 6 June 2024

 DOI: https://doi.org/10.48084/etasr.7798

ABSTRACT

Glaucoma, a progressive eye disease, is a major public concern on health due to its gradual onset and the possibility of irreversible vision loss. Early glaucoma detection is critical because it allows for timely intervention and management, lowering the risk of severe visual impairment. To address this pressing need, we present a comprehensive glaucoma detection methodology that focuses on image processing techniques and machine learning models. The initialization and preprocessing of retinal fundus images obtained from the DRIVE database is the first step in our approach. These images are resized to a standard size, grayscaled, and blurred with Gaussian blur to ensure consistency and noise reduction. Our methodology is built around feature extraction and modeling. We harness the power of deep learning, specifically Long Short-Term Memory (LSTM) and Convolutional Neural Networks (CNNs), which we integrate seamlessly with multi-class Support Vector Machines (SVMs). This synergy enables our Deep Flex SVM-MC model to capture intricate data patterns during training while also demonstrating exceptional adaptability in multi-class classification tasks. The proposed model has a glaucoma detection accuracy of 97.2%, an exceptional sensitivity of 97.53%, indicating its proficiency in correctly identifying glaucoma cases, and a specificity of 96.4%.

Keywords-glaucoma; retinal fundus image; Long Short-Term Memory (LSTM); Convolutional Neural Network (CNN); multi-class SVM; Deep Flex SVM-MC; feature extraction; Histogram of Oriented Gradients (HOG)

I. INTRODUCTION

Glaucoma, a progressive and frequently asymptomatic eye disease, has become a significant health challenge globally. [1]. It is distinguished by optic nerve damage and loss of visual field, and if left undiagnosed or untreated, it may lead to irreversible vision loss [2]. Detection of glaucoma at early stage is critical because it allows for timely intervention and management, lowering the risk of severe visual impairment [3-5]. However, the stealthy nature of glaucoma makes early detection difficult, emphasizing the need for advanced and precise detection methods [6]. Detecting glaucoma early allows for proactive treatment and lifestyle changes to slow or stop the disease's progression, preserving the patient's vision and quality of life [7-8]. To address the challenge of early glaucoma detection, the proposed methodology makes use of the synergy between computer vision and Machine Learning (ML). It starts with preprocessing retinal fundus images from the DRIVE database [18] to ensure uniformity and noise reduction [21]. The methodology's heart is in feature extraction and modelling, where advanced techniques like Histogram of Oriented Gradients (HOG) are used to capture local gradient information and statistical measures. The development of the proposed Deep Flex SVM-MC model is the current paper's most notable contribution. Deep Learning (DL), specifically LSTM and CNN, are seamlessly integrated into this innovative model, which replaces traditional multi-class Support Vector Machines (SVMs). The addition of LSTM-CNN improves the model's ability to capture intricate data patterns during both training and testing, resulting in significantly improved accuracy in multi-class classification, including glaucoma detection.

II. RELATED WORKS

Researchers have recently focused on the detection and classification of glaucoma from retinal fundus images, with the goal of improving accuracy and efficiency by utilizing the most recent DL approaches.

The proposed methodology in [9] used the Spectralis Method and reported a specificity rate of only 88.9%. Authors in [10] used an ensemble approach in 2019 to develop a glaucoma detection model with an 88% accuracy. To address

this limitation, ensemble methods could be improved by experimenting with different combination strategies and taking into account a larger ensemble of diverse models. Authors in [11] established a system model based on the use of various CNN architectures in 2019 and achieved a 96.27% accuracy. For further validation and applicability in real-world scenarios, the dataset size and generalizability limitations should be considered. Authors in [12] projected an automated type of glaucoma detection device based on DWT and also median filter for pre-processing in 2020 and achieved 96.7% accuracy. In [13], an ensemble method based on CNN architecture ResNet was developed and achieved 91.1% accuracy. Authors in [14] proposed GlaucomaNet in 2022, with the model consisting of two CNNs and achieving an accuracy of 93%. The limitation of the work is low accuracy, considering the state-of-the-art.

III. THE PROPOSED SYSTEM

Figure 1 depicts the proposed methodology for Glaucoma Detection on Retinal Fundus Images, which is a comprehensive and systematic approach aimed at accurately identifying glaucoma-related abnormalities. It begins with the Initialization and Preprocessing phases, in which images from the dataset are manipulated. Fundus images are loaded from the DRIVE database [18] and are subjected to various enhancement steps to optimize image quality, such as resizing, grayscale conversion, and Gaussian blur application.

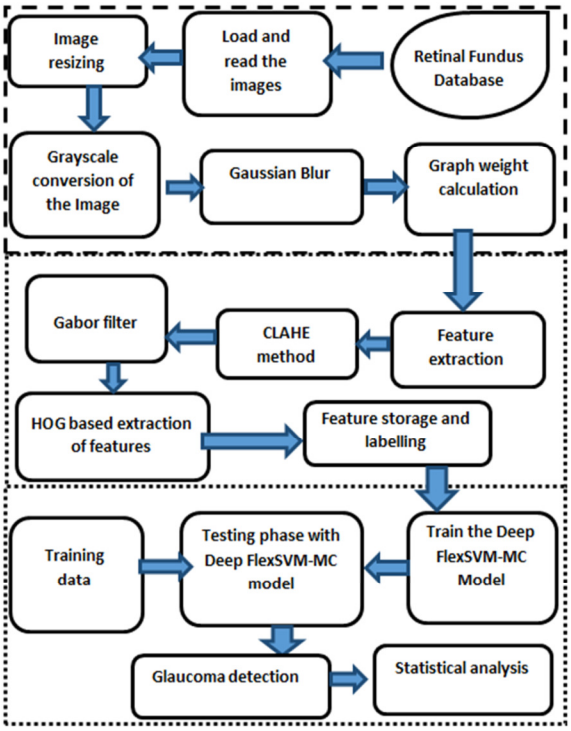

Fig. 1. Block diagram of the proposed glaucoma detection methodology.

The images are then convolved with these filters to produce a set of filtered images, each capturing information at a different orientation and scale [19-21].

When applying Gabor filtering to the enhanced grayscale image G(x, y)' typically a bank of Gabor filters with varying orientations and scales is created [15-17]. The mathematical equation for convolving the image with a Gabor filter F(x, y) at a specific orientation and scale is given by:

$$Filtered(x,y) = G(x,y)' * F(x,y$$

The Deep FlexSVM-MC Model is introduced in the training and testing phases of this methodology. The proposed Deep Flex SVM-MC model, contains various (one input, two convolution, two max pooling, one LSTM, one fully connected) layers. The model starts with the pre-processed test images in the Input Layer and produces. This model combines the power of SVMs with DL, with feature integration handled by LSTM-based CNN. Deep Flex SVM-MC is highly adaptable, allowing for the seamless switching between optimization methods (QP, SMO) based on the characteristics of the dataset, ensuring optimal performance across diverse multi-class classification scenarios. Its adaptability and DL integration make it ideal for multi-class classification tasks in a variety of domains, allowing users to leverage the benefits of DL within the traditional SVM framework and achieve cutting-edge performance

The Deep FlexSVM-MC Model is a robust framework that produces glaucoma detection results. The following Algorithm shows the basic steps of the model.

```
Step 1: Model Initialization
Initialize Deep FlexSVM-MC model with
LSTM-CNN and SVM components
Step 2: Training Phase
For each image in the dataset:
    // Extract HOG features
   // Train LSTM-CNN
  // Define LSTM-CNN layers and
architecture
 // Convolutional Layer 1
  // Max Pooling Layer 1
 // Convolutional Layer 2
     //Max Pooling Layer
     // LSTM Layer - Number of units: 128
     // Fully Connected Layer
     // Output Layer
    //Specify hyper parameters
   // Input: HOG features
    //Output: Features after LSTM-CNN
layers
      Step 2: Train SVM classifier
              // Define SVM parameters
            //Input: Output from LSTM-CNN
           // Output: Trained SVM model
      Step 3: Testing Phase
           // Select a test image
         // Pre-process the test image
        // Resize and convert to
grayscale
        // Extract HOG features from the
test image
```

```
      Step 4: Classify using the model
        //Output = Deep FlexSVM-MC (Output
from LSTM-CNN)
       // Display the classification
result
      Step 5: Glaucoma Detection
(Segmentation)
       // Load a sample image for glaucoma
detection
     // Perform image processing and
segmentation
     // Define segmentation techniques
    // Input: Test image
   // Output: Segmented glaucoma-related
regions
   Step 6: Display intermediate and final
segmentation results
  End
```

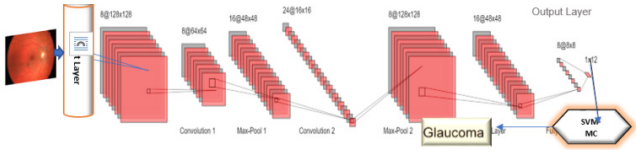

Fig. 2. Proposed model architecture.

We can compute various statistical measures for the considered features, such as mean, variance, skewness, kurtosis, entropy, and energy.

Mean of HOG features (μ): The mean is calculated by summing up all the HOG feature values and dividing by the total number of features (N):

$$\mu = \left(\frac{1}{N}\right) * \Sigma\, HOG_{feature} \quad (1)$$

Variance of HOG Features (σ^2): The variance measures the spread or dispersion of the feature values:

$$\sigma^2 = \left(\frac{1}{N}\right) * \Sigma \left(HOG_{feature} - \mu\right)^2 \quad (2)$$

Skewness of HOG Features (γ): Skewness measures the asymmetry of the feature distribution:

$$\gamma = \left(\frac{1}{N}\right) * \Sigma \left(\frac{\left(HOG_{feature} - \mu\right)^3}{\sigma^3}\right) \quad (3)$$

Kurtosis of HOG Features (κ): Kurtosis measures the "tailedness" or peakedness of the feature distribution:

$$\kappa = \left(\frac{1}{N}\right) * \Sigma \left(\frac{\left(HOG_{feature} - \mu\right)^4}{\sigma^4}\right) - 3 \quad (4)$$

Entropy of HOG Features (E): Entropy measures the information content or uncertainty in the feature distribution:

$$E = -\Sigma \left(P\left(HOG_{feature}\right) * log2\left(P\left(HOG_{feature}\right)\right)\right) (5)$$

where $P(HOG_{feature})$ is the probability of observing a particular HOG feature.

Energy of HOG Features (E): Energy is a measure of the magnitude or strength of the feature distribution:

$$E = \Sigma\, (HOG_{feature}^2) \quad (6)$$

These statistical measures provide information about the HOG feature distribution's central tendency, spread, symmetry, and information content.

IV. RESULTS AND DISCUSSION

Figure 3, sourced directly from the renowned DRIVE database of retinal fundus images, serves as the foundation of our analysis. Figure 4 shows the result of resizing the original image, Figure 5 shows the result of grayscale conversion by isolating the green channel, and Figure 6 shows the isolated background of the image.

Figure 7 shows the outcome of Gaussian blur application to the grayscale image. This improved image quality significantly improves the effectiveness of the subsequent processing stages. Figure 8 shows the image after it has been subjected to Contrast Limited Adaptive Histogram Equalisation (CLAHE). Figure 9 is an extracted Region of Interest (ROI) encompassing the optical disc, a key anatomical feature in our research.

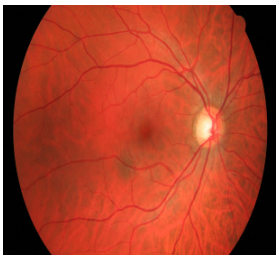

Fig. 3. Original image.

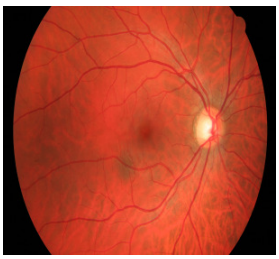

Fig. 4. Resized image.

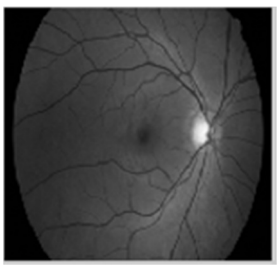

Fig. 5. Green channel image.

Fig. 6. Image background.

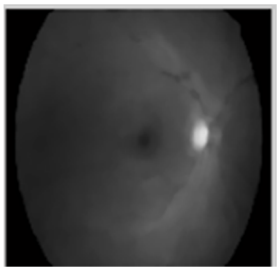

Fig. 7. Gaussian blurred image.

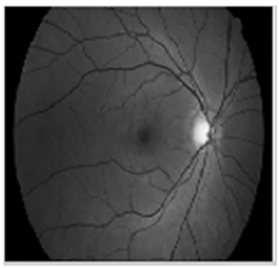

Fig. 8. Image after CLAHE application.

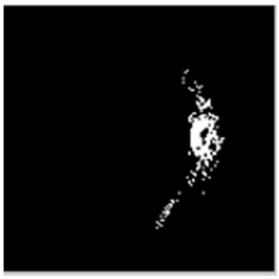

Fig. 9. Extracted optical disc region.

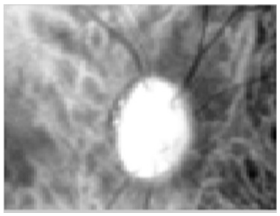

Fig. 10. Vessel extracted image for feature extraction using HoG.

Figure 10 shows an image that has been vessel segmented, effectively isolating blood vessels within retinal images. Figure 11 depicts the end result of our segmentation efforts, emphasising and highlighting both the optic cup and the optic disc. Figure 12 shows the glaucoma affected regions via superimposition of vessels segmented on the original image. Figure 13 highlights the final optic disk region for detection of the affected part.

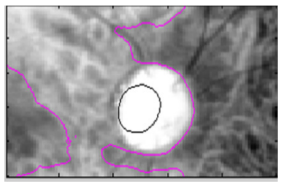

Fig. 11. Final segmented region highlighting the optic cup and optic disc.

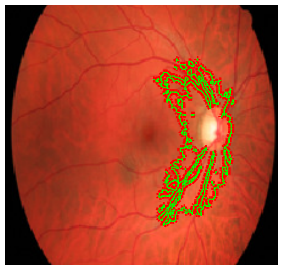

Fig. 12. Glaucoma affected regions.

Fig. 13. Final optic disk region for glaucoma detection.

A. Accuracy

The accuracy metric counts how many correct predictions were made out of all the predictions made.

$$\text{Accuracy} = \frac{(\text{TP}+\text{TN})}{\text{TP}+\text{FP}+\text{TN}+\text{FN}} \quad (7)$$

where TP stands for True Positive, TN for True Negative, FP for False Positive, and FN for False Negative.

TABLE I. ACCURACY COMPARISON

Method	**Accuracy (%)**
CNN [12]	96.27
FA-DWT [13]	96.7
ResNet [14]	91.1
GlaucomaNet [15]	93
CNN (AlexNet) + RF [18]	93.33
K-Means [19]	92
Proposed	**97.2**

The accuracy comparison of the proposed method with other works in the context of glaucoma detection is presented in Table I and Figure 14. The proposed method achieves a remarkable accuracy of 97.2%, demonstrating its ability to correctly classify glaucoma cases. The proposed method

outperforms ResNet, GlaucomaNet, and even ensemble approaches such as CNN (AlexNet) + Random Forest (RF), implying that it addresses specific glaucoma detection challenges.

B. Sensitivity

Sensitivity, a critical metric in medical diagnostics, assesses the model's ability to detect positive cases, in this case, glaucoma, among all actual positive cases.

$$\text{Sensitivity} = \frac{\text{TP}}{\text{TP+ FN}} \quad (8)$$

Table II and Figure 15 show the sensitivity analysis result comparison with existing works, with a particular emphasis on the performance of the proposed Deep FlexSVM-MC Model. The proposed model has a sensitivity of 97.53%, indicating an exceptional ability to correctly identify glaucoma cases. This visual representation clearly shows that the proposed Deep FlexSVM-MC Model outperforms the established methods and DL architectures in glaucoma detection, with a sensitivity rate of 97.53%.

TABLE II. SENSITIVITY COMPARISON

Method	Sensitivity (%)
Spectralis [10]	53
ResNet [14]	91.1
DRUNET [16]	92
Basic CNN models [17]	87
K-Means [19]	93
Proposed	**97.53**

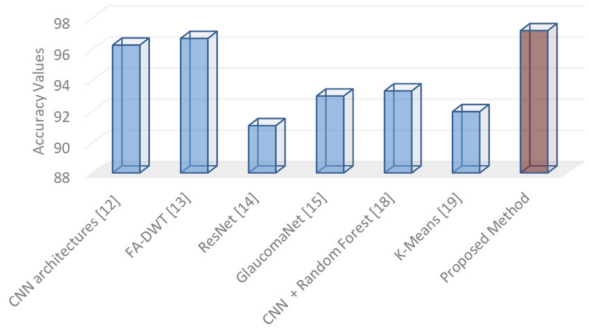

Fig. 14. Accuracy comparison.

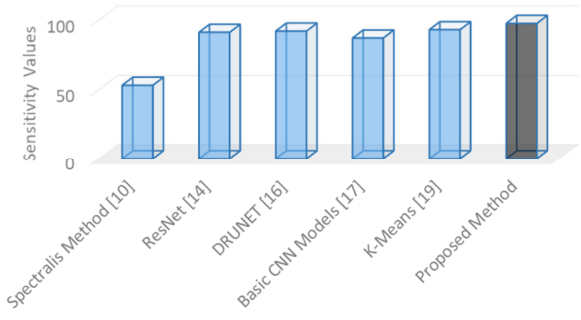

Fig. 15. Sensitivity comparison.

C. Specificity

Specificity assesses model's ability to identify correctly the negative instances (in this case, healthy images).

$$\text{Specificity} = \frac{\text{TN}}{\text{(FP+ TN)}} \quad (9)$$

Table III and Figure 16 show the specificity analysis result comparison with existing works.

The proposed model has attained a specificity of 96.4%, indicating a high ability to correctly classify healthy individuals as non-glaucomatous. The Spectralis Method comes closest among the other methods, with a specificity of 95.6%, demonstrating a comparable level of performance in this regard.

TABLE III. SPECIFICITY COMPARISON

Methods	Specificity (%)
Spectralis [10]	95.6
ResNet [14]	83.3
Basic CNN models [17]	89
K-Means [19]	93
Automated System [20]	94
Proposed	**96.4**

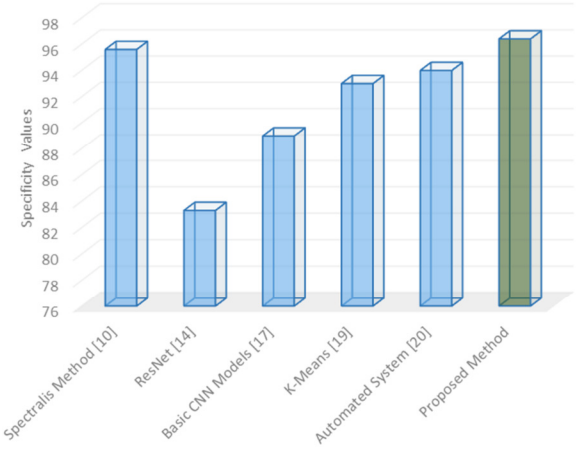

Fig. 16. Specificity comparison.

D. Discussion

As evidenced by its remarkable performance metrics, the proposed Deep Flex SVM-MC Model excels in glaucoma detection. It achieves 97.2% accuracy, demonstrating its ability to correctly classify glaucoma cases with a high degree of accuracy. Furthermore, the model has an exceptional sensitivity rate of 97.53%, demonstrating its ability to identify true positive glaucoma cases and a specificity rate of 96.4%.

V. CONCLUSION

Our method includes the initialization and preprocessing of retinal fundus images, advanced feature extraction by using Histogram Oriented Gradients, and the creation of the proposed Deep Flex SVM-MC model, which seamlessly integrates deep learning (LSTM-CNN) with traditional Multi-Class Support

Vector Machines. Our study's findings are very encouraging, with the Deep Flex SVM-MC model achieving exceptional performance metrics. It achieves an impressive accuracy rate of 97.2%. Furthermore, it has a high sensitivity of 97.53%, indicating its ability to identify true positive glaucoma cases, which is critical for early diagnosis. Furthermore, the model has a specificity of 96.4%, demonstrating its ability distinguish between healthy and glaucoma patients.

REFERENCES

[1] S. P. Mariotti, *Global data on visual impairments 2010*. Geneva, Switzerland: World Health Organization, 2012.

[2] J. Flammer, *Glaucoma : a guide for patients, an introduction for care-providers, a quick reference*. Bern, Switzerland: Hogrefe & Huber, 2003.

[3] F. Badala, K. Nouri-Mahdavi, D. A. Raoof, N. Leeprechanon, S. K. Law, and J. Caprioli, "Optic Disk and Nerve Fiber Layer Imaging to Detect Glaucoma," *American Journal of Ophthalmology*, vol. 144, no. 5, pp. 724–732, Nov. 2007, https://doi.org/10.1016/j.ajo.2007.07.010.

[4] A. Osareh, M. Mirmehdi, B. Thomas, and R. Markham, "Automated identification of diabetic retinal exudates in digital colour images," *British Journal of Ophthalmology*, vol. 87, no. 10, pp. 1220–1223, Oct. 2003.

[5] D. Pascolini and S. P. Mariotti, "Global estimates of visual impairment: 2010," *British Journal of Ophthalmology*, vol. 96, no. 5, pp. 614–618, May 2012, https://doi.org/10.1136/bjophthalmol-2011-300539.

[6] S. J. K. Pedersen, *Circular Hough Transform*. Aalborg, Denmark: Aalborg University, 2007.

[7] C. Sinthanayothin, J. F. Boyce, H. L. Cook, and T. H. Williamson, "Automated localisation of the optic disc, fovea, and retinal blood vessels from digital colour fundus images," *British Journal of Ophthalmology*, vol. 83, no. 8, pp. 902–910, Aug. 1999, https://doi.org/10.1136/bjo.83.8.902.

[8] J. C. Bezdek, J. Keller, R. Krisnapuram, and N. Pal, *Fuzzy Models and Algorithms for Pattern Recognition and Image Processing*. Amsterdam, Netherlands: Kluwer Academic Publishers, 1999.

[9] M. Nieves-Moreno *et al.*, "New Normative Database of Inner Macular Layer Thickness Measured by Spectralis OCT Used as Reference Standard for Glaucoma Detection," *Translational Vision Science & Technology*, vol. 7, no. 1, Feb. 2018, Art. no. 20, https://doi.org/10.1167/tvst.7.1.20.

[10] S. Serte and A. Serener, "A Generalized Deep Learning Model for Glaucoma Detection," in *3rd International Symposium on Multidisciplinary Studies and Innovative Technologies*, Ankara, Turkey, Oct. 2019, pp. 1–5, https://doi.org/10.1109/ISMSIT.2019.8932753.

[11] K. A. Thakoor, X. Li, E. Tsamis, P. Sajda, and D. C. Hood, "Enhancing the Accuracy of Glaucoma Detection from OCT Probability Maps using Convolutional Neural Networks," in *41st Annual International Conference of the IEEE Engineering in Medicine and Biology Society*, Berlin, Germany, Jul. 2019, pp. 2036–2040, https://doi.org/10.1109/EMBC.2019.8856899.

[12] L. Abdel-Hamid, "Glaucoma Detection from Retinal Images Using Statistical and Textural Wavelet Features," *Journal of Digital Imaging*, vol. 33, no. 1, pp. 151–158, Feb. 2020, https://doi.org/10.1007/s10278-019-00189-0.

[13] P. K. Chaudhary and R. B. Pachori, "Automatic diagnosis of glaucoma using two-dimensional Fourier-Bessel series expansion based empirical wavelet transform," *Biomedical Signal Processing and Control*, vol. 64, Feb. 2021, Art. no. 102237, https://doi.org/10.1016/j.bspc.2020.102237.

[14] M. Lin *et al.*, "Automated diagnosing primary open-angle glaucoma from fundus image by simulating human's grading with deep learning," *Scientific Reports*, vol. 12, no. 1, Aug. 2022, Art. no. 14080, https://doi.org/10.1038/s41598-022-17753-4.

[15] H. Muhammad *et al.*, "Hybrid Deep Learning on Single Wide-field Optical Coherence tomography Scans Accurately Classifies Glaucoma Suspects," *Journal of Glaucoma*, vol. 26, no. 12, pp. 1086–1094, Dec. 2017, https://doi.org/10.1097/IJG.0000000000000765.

[16] J. Ayub *et al.*, "Glaucoma detection through optic disc and cup segmentation using K-mean clustering," in *International Conference on Computing, Electronic and Electrical Engineering*, Quetta, Pakistan, Apr. 2016, pp. 143–147, https://doi.org/10.1109/ICECUBE.2016.7495212.

[17] A. Mvoulana, R. Kachouri, and M. Akil, "Fully automated method for glaucoma screening using robust optic nerve head detection and unsupervised segmentation based cup-to-disc ratio computation in retinal fundus images," *Computerized Medical Imaging and Graphics*, vol. 77, Oct. 2019, Art. no. 101643, https://doi.org/10.1016/j.compmedimag.2019.101643.

[18] "DRIVE: Digital Retinal Images for Vessel Extraction." https://drive.grand-challenge.org/DRIVE/.

[19] N. Bourkache, M. Laghrouch, and S. Sidhom, "Gabor Filter Algorithm for medical image processing: evolution in Big Data context," in *International Multi-Conference on: "Organization of Knowledge and Advanced Technologies" (OCTA)*, Tunis, Tunisia, Feb. 2020, pp. 1–4, https://doi.org/10.1109/OCTA49274.2020.9151681.

[20] D. Gabor, "Theory of communication," *Journal of the IEEE*, vol. 93, pp. 429–441, Nov. 1946.

[21] M. Kunt and T. Ebrahimi, "Image compression by Gabor expansion," *Optical Engineering*, vol. 30, no. 7, pp. 873–880, Jul. 1991, https://doi.org/10.1117/12.55898.